

# Study on Array Source Stirring Reverberation Chamber

Wenxing Li, Chongyi Yue, and Wenhua Yu

Department of Information and Communication Engineering  
Harbin Engineering University, Harbin, 150001, China  
liwenxing@hrbeu.edu.cn, yuechongyi@hrbeu.edu.cn, wenyu2comu@gmail.com

**Abstract** — Because the structure of transmitting antenna significantly affects the performance of source stirred reverberation chamber, a source stirring reverberation chamber excited by antenna array with a novel configuration is proposed and investigated in this paper. In contrast to traditional source stirring techniques, fewer array elements in reasonable arrangement are employed to use the test space efficiently and ensure the desired field characteristics, such as uniform statistics, isotropic and random polarization. Numerical experiments demonstrate that the statistical distribution of electrical field meets Standard IEC 61000-4-21 and has advantage over the traditional stirring systems.

**Index Terms** — Array antenna, Chi-square test, reverberation chamber, source stirring technique.

## I. INTRODUCTION

Compared with traditional EMC test facilities, the Reverberation Chamber (RC) is a new kind of EMC test facility with advantages in construction cost and dynamic range. Better electric field intensity using the same input power and accurate results can be obtained in RC. More attentions have been attracted to RCs and the related research has become one of the hottest research topics today [1-4]. A RC usually consists of a shielding cavity, transmitting antenna, receiving antenna, field probe and stirring device(s), which has characteristics of statistical homogeneity, isotropy and random polarization [5]. Both radiation sensitivity and shielding performance tests can be conducted in the chamber.

The mechanical stirred RC is first reported [6] and widely used in both industrial and academic research. The stirring relies on rotation of metal plates in irregular shapes, which make the operation

and installation complicated and available space relatively small for EUT (equipment under test) [7,8]. In order to tackle this problem, the existing source-stirred RC [8] requires a mobile transmitting antenna on the ground. It does simplify the structure of reverberation chamber, but it is difficult or impossible to obtain the random changes of antenna positions and ensure the independence between different states of stirring. Meanwhile, the manual processing on the antenna may decrease accuracy and efficiency. To overcome this shortage, a source-stirred method is proposed by exciting multiple antennas at different times [9], which needs to employ several independent transmitting antennas. The electric field distribution will be changed when different antennas are excited. However, these independent transmitting antennas occupy a large cavity space and increase the construction cost.

To resolve this contradiction, a source stirring method via an array antenna is proposed [10]. Four array elements are mounted on each surface of a hexahedral structure and this structure is located on the ground. Different elements of array are motivated separately to stir the chamber. The source stirring method via an antenna array can obtain larger EUT space and guarantees independence of electric field distributions on different stirring steps. But this antenna array in a hexahedral pattern still occupies a large space in the chamber and reduces the area available for EUT.

Aiming at the issues above, a reverberation chamber stirred by a novel antenna array is developed in this paper, and the planar array is distributed near the chamber wall. This antenna array includes twelve array elements, three of which are excited simultaneously on each stirring step. This design reduces the volume occupied by

transmitting antenna array and has a simple structure with small quantity of array elements. In addition, this design is also satisfied with the requirements of the number of stirring steps and independence in different stirring states.

## II. SOURCE-STIRRED TECHNIQUE ANALYSIS

The electric field density inside a source-stirred chamber is associated with both position and orientation of transmitting antenna. The inhomogeneous wave in a chamber satisfies the following equation:

$$\nabla \mathbf{E} + \omega^2 \mu_0 \varepsilon_0 \mathbf{E} = j\omega \mu_0 \mathbf{J}. \quad (1)$$

The eigen solution of (1) is expressed as:

$$\begin{cases} E_x = \cos \frac{m\pi x}{L} \sin \frac{n\pi y}{W} \sin \frac{p\pi z}{H} \\ E_y = \sin \frac{m\pi x}{L} \cos \frac{n\pi y}{W} \sin \frac{p\pi z}{H} \\ E_z = \sin \frac{m\pi x}{L} \sin \frac{n\pi y}{W} \cos \frac{p\pi z}{H}, \end{cases} \quad (2)$$

where  $L$ ,  $W$  and  $H$  represent the length, width and height of chamber, respectively; and  $m$ ,  $n$  and  $p$  are mode numbers,

$$\left[ \left( \frac{m\pi}{L} \right)^2 + \left( \frac{n\pi}{W} \right)^2 + \left( \frac{p\pi}{H} \right)^2 \right] = k_{mnp}^2. \quad (3)$$

The resonant frequency of source-stirred chamber can be expressed as:

$$\begin{aligned} f_{mnp} &= \frac{k_{mnp}}{2\pi\sqrt{\mu_0\varepsilon_0}} \\ &= \frac{c_0}{2} \sqrt{\left( \frac{m}{L} \right)^2 + \left( \frac{n}{W} \right)^2 + \left( \frac{p}{H} \right)^2}. \end{aligned} \quad (4)$$

If  $A_{m'np}$ ,  $A_{mn'p}$  and  $A_{mnp'}$  are mode values, the electrical field components  $E_x$ ,  $E_y$  and  $E_z$  inside the chamber can be expressed as:

$$\begin{aligned} \mathbf{E} &= \sum_{m,n,p} (c_{xmp} A_{m'np} \hat{e}_x \\ &\quad + c_{ymp} A_{mn'p} \hat{e}_y + c_{zmp} A_{mnp'} \hat{e}_z), \end{aligned} \quad (5)$$

where  $c_{xmp}$ ,  $c_{ymp}$  and  $c_{zmp}$  can be obtained by [11]:

$$\begin{aligned} c_{xmp} &= \frac{c^2}{4\pi^2 (f^2 - f_{mnp}^2)} \frac{8}{LWH} \\ &\quad \iiint j\omega \mu_0 J_x A_{m'np} dx dy dz \\ c_{ymp} &= \frac{c^2}{4\pi^2 (f^2 - f_{mnp}^2)} \frac{8}{LWH} \\ &\quad \iiint j\omega \mu_0 J_y A_{mn'p} dx dy dz \\ c_{zmp} &= \frac{c^2}{4\pi^2 (f^2 - f_{mnp}^2)} \frac{8}{LWH} \\ &\quad \iiint j\omega \mu_0 J_z A_{mnp'} dx dy dz, \end{aligned} \quad (6)$$

where  $J_x$ ,  $J_y$  and  $J_z$  are components of the current density vector. From (5) and (6), both position and orientation of transmitting antenna will influence the field in the cavity. For an antenna array in the chamber, both position and orientation of array elements are different from each other. Motivating different elements at different times can change the field distributions in the chamber. When an antenna array has sufficient emission states, a field distribution of statistical uniformity can be formed during a stirring period.

## III. ARRAY ANTENNA DESIGN

### A. The lowest usable frequency

The Lowest Usable Frequency (LUF) of reverberation chamber refers to the lowest available frequency of EMC test in the chamber, which is an important indicator of RC. The dimensions of the chamber in this paper are selected to be  $L=4,000$  mm,  $W=2,480$  mm and  $H=3,000$  m, which determine  $f_0=62.5$  MHz (the lowest resonant frequency) and  $f_{LUF}=3f_0$ . The variation of mode number and density with frequency can be expressed as [11]:

$$N(f) \approx \frac{8\pi}{3} LWH \left( \frac{f}{c_0} \right)^3 - (L+W+H) \frac{f}{c_0} + \frac{1}{2}, \quad (7)$$

$$\frac{\partial N}{\partial f} \approx 8\pi LWH \frac{f^2}{c_0^3} - (L+W+H) \frac{1}{c_0}. \quad (8)$$

The chamber will have a good performance at the mode quantity of 100 or mode density of 1.5 Mode/MHz. It is observed from Fig. 1 that the quantity of mode increases linearly with frequency. The number of mode in the chamber reaches 100 at the frequency of 230 MHz, and the mode density qualifies the requirement of 1.5 modes/MHz at the frequency of 235 MHz. The reverberation chamber can perform well at the frequency of 235 MHz and above. It is indicated from Fig. 2 that with increasing of frequency, the gap between two modes is getting smaller, which means the field uniformity is getting better as the frequency increases. The change of modal gap between two adjacent modes is shown in Fig. 2.

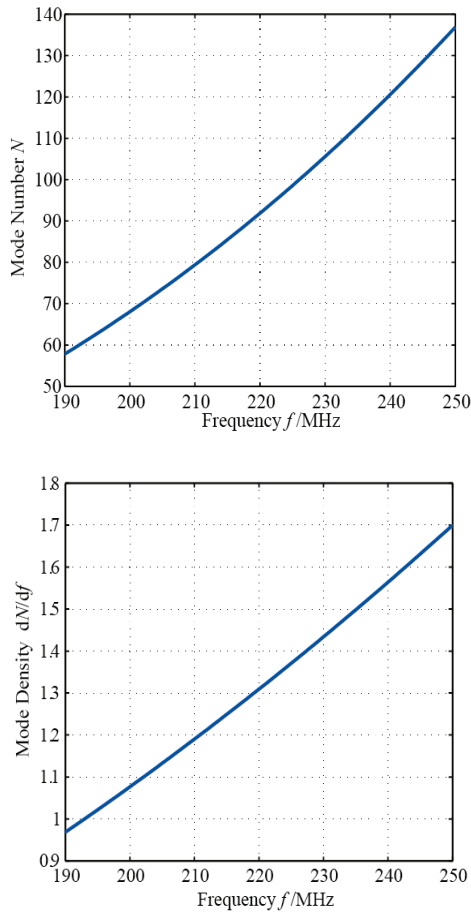


Fig. 1. Variation of mode number and mode density with frequency.

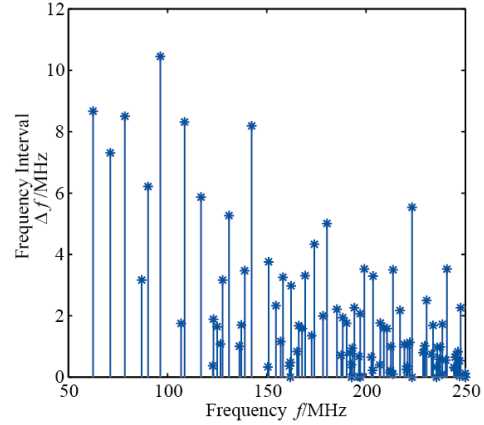


Fig. 2. Modal gap in the source-stirred chamber.

## B. The design of array antenna

In order to get an insight into the coupling mechanism between antenna array and the chamber, and to reduce the impact caused by the structure of antenna on the field distribution, a half-wave dipole is chosen to be an array element in this paper. The maximum likelihood estimation method and the given confidence level are considered to decide the number of stirring steps, which is the same as the sampling size of electric field when the array antenna is designed. Electrical field in cavity obeys Rayleigh distribution, whose PDF can be deduced as:

$$f(E_i) = \frac{E_i}{\sigma^2} e^{-\frac{E_i^2}{2\sigma^2}}, \quad (9)$$

where  $i$  represents  $x$ ,  $y$  or  $z$ . Using the maximum likelihood estimation can get the estimator as:

$$\hat{\sigma}^2 = \frac{1}{2n} \sum_{j=1}^n E_{ij} = \frac{\overline{E_i^2}}{2}. \quad (10)$$

If the sampling number  $n$  is sufficiently large, the estimator  $\hat{\sigma}^2$  will be the normal distribution, and the variance is:

$$\text{var}[\hat{\sigma}^2] = \left\{ -nE \left[ \frac{\partial^2 \ln f}{\partial (\sigma^2)^2} \right] \right\}^{-1} = \frac{\sigma^4}{n}, \quad (11)$$

where  $E$  is an expected value and  $f$  is the function in (9). After normalizing  $\hat{\sigma}^2$ , the normalized confidence interval is expressed as:

$$d(\text{dB}) = 10 \log \frac{1+k/\sqrt{n}}{1-k/\sqrt{n}}, \quad (12)$$

and the sample size can be derived as:

$$n = k^2 \left( \frac{10^{d/10} + 1}{10^{d/10} - 1} \right)^2. \quad (13)$$

We choose  $d$ , ideal confidence level,  $k$  and number of samples to be 1 dB, 90%, 1.65 and 207, respectively [12].

Based on the discussions above, 207 stirring steps can reach the ideal confidence level. Enough stirring steps can be obtained by exciting different combination of elements of the array at each time. 66, 220 or 495 stirring steps can be achieved when 2, 3 or 4 array elements are excited at each time. Obviously, 3 elements and 220 stirring steps is enough for sample size, which is calculated in (13). Therefore, as different elements are excited, 220 emission statuses are achieved by exciting different combinations. It is indicated in Fig. 3 how the elements are motivated in the array, where white and black points represent active elements and non-active elements, respectively.

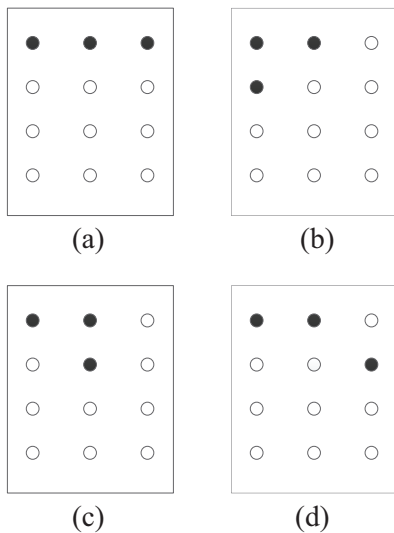


Fig. 3. Excitation configuration of array antennas.

The spacing between adjacent elements also has significant influence on the field distribution in the cavity. For the sake of good statistical distribution of electric field samples, the field independence of different stirring steps is an important factor to determine the configuration of array elements. According to the plane wave spectrum [13], the correlation function of field

intensity in a reverberation chamber is:

$$\rho(\mathbf{r}_1, \mathbf{r}_2) = \frac{\langle \mathbf{E}(\mathbf{r}_1) \mathbf{E}^*(\mathbf{r}_2) \rangle}{\sqrt{\langle |\mathbf{E}(\mathbf{r}_1)|^2 \rangle \langle |\mathbf{E}(\mathbf{r}_2)|^2 \rangle}}, \quad (14)$$

where  $\mathbf{r}_1$  and  $\mathbf{r}_2$  are two position vectors, and a simplified formulation is given as:

$$\rho(\mathbf{r}_1, \mathbf{r}_2) = \frac{\sin(k|\mathbf{r}_1 - \mathbf{r}_2|)}{k|\mathbf{r}_1 - \mathbf{r}_2|}. \quad (15)$$

We can see from (15) that the minimization distance of adjacent elements for the relevant function  $\rho=0$  is  $\lambda/2$ , which ensures the independence of different field samples. The orientation of elements is random but should be neither parallel to each other nor parallel to the chamber wall, which ensures wave to radiate and reflect in different paths to avoid strong mutual coupling. The schematic diagram of arrangement of elements is shown in Fig. 4, where the distance between adjacent elements is  $\lambda/2$  and the orientation of elements is different from each other.

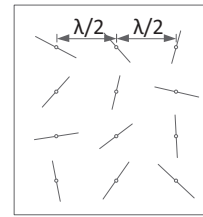


Fig. 4. Schematic diagram of array antenna.

In conclusion, the maximum wavelength is  $\lambda=1.58\text{m}$  in frequency band over 190 MHz to 250 MHz. The distance between the antenna array and the chamber wall is  $\lambda \approx 0.4\text{m}$ , and twelve elements of different orientations are distributed in a plane with distance of  $\lambda/2$  from each other. The simulation model of this source-stirred reverberation chamber is shown in Fig. 5.

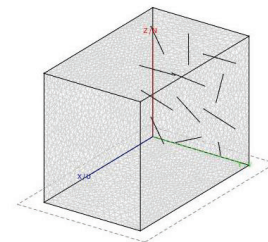


Fig. 5. Simulation model of source-stirred chamber.

### C. The utilization of EUT area

The planar array antenna in this paper takes little space of cavity so that most of the space can be used to conduct EMC test, which effectively improves the space utilization of the cavity. It is shown in Table 1 the comparison of utilization ratio of cavity space between different reverberation chambers.

Table 1: The comparison of utilization ratio of cavity

Type of Chamber	Volume of Cavity (m <sup>3</sup> )	Spatial Volume for EUT (m <sup>3</sup> )	Utilization Ratio of Cavity
Mechanical stirred RC [14]	22.475	9.61	42.76%
Source-stirred RC [15]	130.416	30.525	23.41%
Source-stirred RC [16]	60	26.25	43.75%
Source-stirred RC in this paper	29.76	14.92	50.14%

The volume of the cavity refers to the inner spatial volume in the reverberation chamber, and the volume of space for EUT is calculated according to IEC61000-4-21. The ratio of spatial volume for EUT to the volume of the cavity is utilization ratio of cavity. It is indicated that the utilization ratio of cavity of chamber designed in this paper is bigger than that in mechanical stirred chamber and other source-stirred chambers, which means that the chamber designed in this paper can be used for bigger EUT test if the volume of all the chambers are the same.

## IV. SIMULATION TESTS AND RESULTS

### A. Establishment and controlling of simulation model

The simulation of source-stirred reverberation chamber has the following characteristics:

(1) The inner volume of cavity is large and mesh generation requires a large amount of computing

resources.

(2) The position and orientation of transmitting antennas are continuously changing.

(3) The conductivity of cavity wall cannot be infinitely large.

(4) The cavity is totally enclosed with multiple resonance points and no electromagnetic energy radiates outside.

According to these characteristics, MoM based FEKO software is chosen as a kernel in this paper. MoM only needs to mesh the cavity wall, which can reduce the burden on computing resources and artificial errors caused by continuous model changing. In addition, this method can deal with good conductor and resonant cavity such as convergence and numerical dispersion, better than other numerical methods.

Then the array antenna is arranged in one side of the cavity and the other side is reserved for the EUT. Two observation points are chosen in the EUT area and electrical field data on these points are used to analyze the field distribution inside the cavity. The coordinates of eight vertices (A~D, A'~D') of working volume and two observation points (P, Q) are shown in Table 2.

Table 2: Coordinates of vertices and observation points

Point	X	y	Z
A	0.8	0.4	0.4
B	0.8	2	0.4
C	3.6	0.4	0.4
D	3.6	2	0.4
A'	0.8	0.4	2.6
B'	0.8	2	2.6
C'	3.6	0.4	2.6
D'	3.6	2	2.6
P	2	1.2	1.4
Q	1.4	1.6	2

Matlab program is used to control the excitation of array antenna as well as save and process sampling data of electric field during the whole stirring procedure in this paper. Different field distributions are formed in the working volume for each excitation, as shown in Fig. 6. Three electric field components at eight vertices of working volume and observation point P and Q are recorded respectively at different stirring status. After a complete stirring period, the recorded data of

electric field is processed to obtain the statistical characteristic of field component samples to compare with theoretical results. The controlling of

the excitation storage of data, both data process and analysis are realized through Matlab, and the flow chart of simulation procedure is shown in Fig. 7.

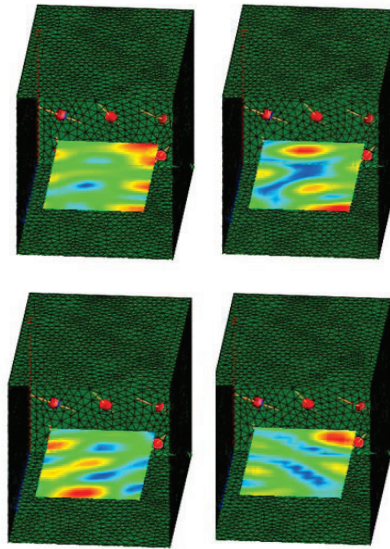


Fig. 6. Variation of electric field of different stirring steps.

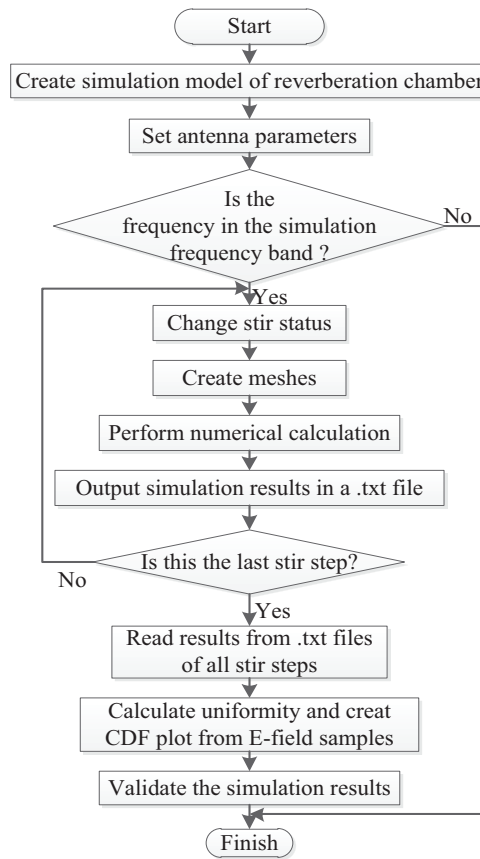


Fig. 7. Flow chart of one complete stirring procedure.

## B. CPU runtime and memory requirements

The computational requirements needed for the simulation of source-stirred reverberation chamber increase as frequency rises, in terms of both the memory needed and the solution time. Therefore, it is useful to estimate the memory and CPU time to complete one simulation run. The memory  $M$  needed for storage of the matrix  $\mathbf{Z}$  in MoM method can be calculated as:

$$M \approx 36N_T^2 + 16N_S^2 \text{ Byte}, \quad (16)$$

where  $N_T$  and  $N_S$  represent the number of triangles and segments respectively. The CUP time for one stirring step can be also estimated as:

$$t \sim O_t(f^{4-6}) + O_s(f^4), \quad (17)$$

which means the time needed for triangles and segments is on the order of  $f^{4-6}$  and  $f^4$  [11], respectively.

Memory requirements and CPU runtime for one stirring step obtained in source-stirred reverberation chamber simulations with FEKO are listed in Table 3.

Table 3: CUP runtime and memory requirements for one frequency and one stirring step

Frequency MHz	$N_T$	Memory MByte	CPU Runtime mm:ss
190	6833	806	08:27
202	7600	996	10:51
217	8633	1266	15:39
229	9563	1547	19:51
238	10633	1873	25:37
247	12030	2322	37:02

## C. Simulation results

After one stirring cycle, the statistical distribution of field samples at the observation point P can be obtained. The comparison between the field component samples and theoretical results is shown in Fig. 8, and the simulation is carried out at 190 MHz with 220 stirring steps in one stirring cycle. It can be seen from Fig. 8 that the simulated and theoretical results are in a good agreement, implying that the field distribution of the stirring period in this source-stirred reverberation chamber obeys Rayleigh distribution [11]. The simulation result of x-component is closer to theoretical one, because the dimension of x-direction in the chamber is larger and the electric field distribution is close to uniform.

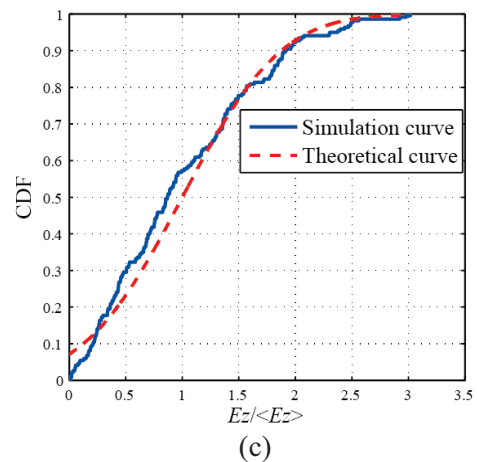
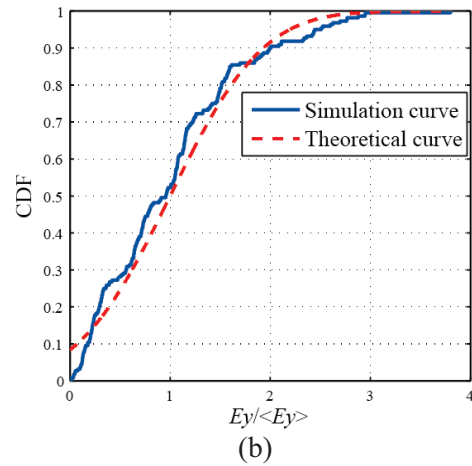
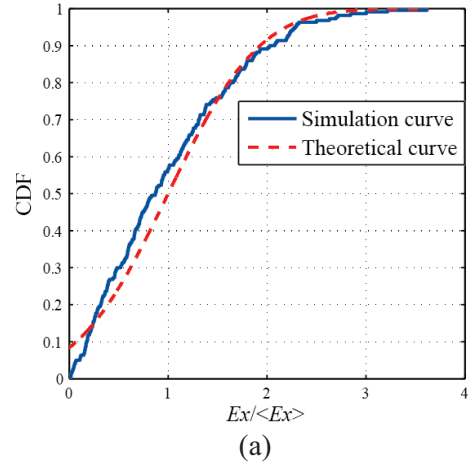


Fig. 8. Simulation and theoretical CDF curves of three electric field components.

In order to verify the fitting degree of theoretical and simulated CDF curves, the Chi-square goodness-of-fit is adopted. The difference

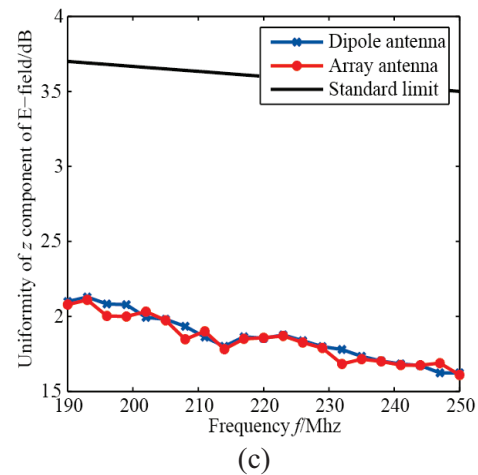
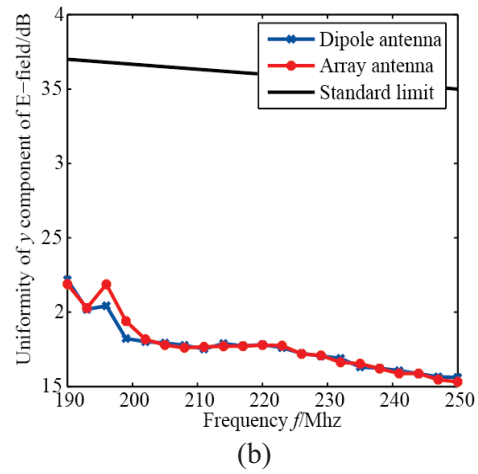
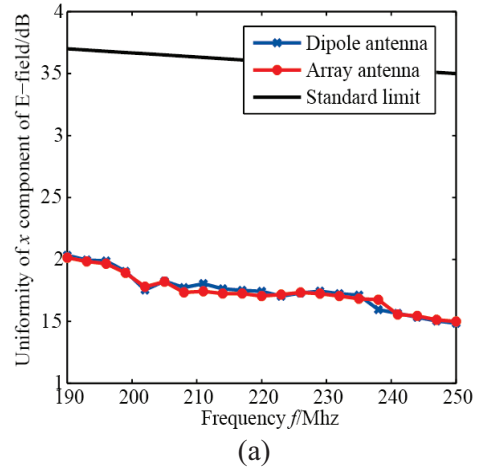
between the observed samples and expected distribution can be defined as:

$$\chi^2 = \sum_{i=1}^n \frac{(o_i - e_i)^2}{e_i}, \quad (18)$$

where  $o_i$  is sampling quantity of the  $i$ th interval, and  $e_i$  is the expected quantity of samples in the  $i$ th interval if the hypothesized distribution is correct. When the sample size turns out to be infinite, the statistic  $\chi^2$  would obey n-p-3 Chi-square distribution of n-p-3 degrees of freedom, in which  $p$  is a parameter in the hypothesized distribution. The  $\chi^2$  can be calculated using (18). If  $\chi^2 < \chi_{(n-p-3)1-\alpha}^2$ , the hypothesized distribution is acceptable.

If the recorded field samples are divided into 10 intervals, the parameter will be 1 and the confidence level will be 0.5. The statistics  $\chi_{E_x}^2$ ,  $\chi_{E_y}^2$  and  $\chi_{E_z}^2$  are 9.941, 11.015 and 10.983, respectively, which are smaller than the threshold value and demonstrates the samples of field component to be Raleigh distribution and the statistically uniform electric field environment in this chamber.

Field uniformity is also an important factor [1, 3] when evaluating the performance of reverberation chamber, and it can be achieved by collecting all the maximum electric field samples at vertices of cubic working volume. The ranges in three directions are  $x=0.8\sim 3.6$  m,  $y=0.4\sim 2$  m and  $z=0.4\sim 2.6$  m. The uniformity of three electric field components and total electric field is shown in Figs. 9 (a)-(d). The blue polyline represents the field uniformity of chamber stirred by a mobile dipole, and the red line represents uniformity of chamber stirred by array antenna. The model of single dipole source-stirring is established to compare the stirring effect between the traditional method and proposed one in this paper, and the dimensions, material of chamber, and the simulation frequency of these two models are the same. The only difference is that the single dipole is moving randomly on the surface.



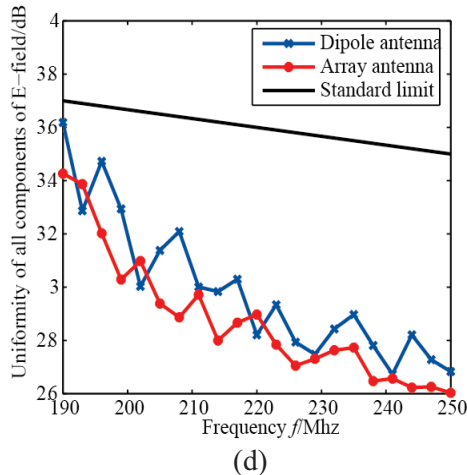


Fig. 9. Uniformity of electric field.

From Figs. 9 (a)-(c), uniformities of three field components are less than 2 dB, and the difference between two curves are not significant. But from Fig. 9 (d), the total field uniformity of array antenna stirring is not only better than that of single mobile dipole stirring, but also closer to the limits on field uniformity in the IEC Standard. Compared with the traditional way of single mobile antenna stirring, the source-stirred technique by array antenna can reduce the standard deviation of field uniformity, namely, a better electromagnetic environment of EMC test can be obtained.

## V. CONCLUSION

A novel type of source-stirred chamber via a planar antenna array is designed in this paper. The composition of the array is uncomplicated and space efficient, which effectively increases the available space for EUT. Matlab is used to control the electromagnetic computational software to realize the stirring automation. The simulation results demonstrate that the simulation CDF distributions of the electric field in the working volume of the chamber is in a good agreement with the theoretical value, and is also validated by Chi-square good-of-fitness test. The electric field uniformity of this antenna array not only meets the IEC61000-4-21 Standard, but also proves that this new source stirring technique is better than traditional ones.

## REFERENCES

- [1] V. Rajamani, C. Bunting, and G. Freyer, "Why consider EMC testing in a reverberation chamber,"

*IEEE Int. Conf. on Electromagnetic Interference & Compatibility*, Bangalore, India, pp. 303-308, November 2008.

- [2] L. De Vries-Venter and D. C. Baker, "EMC radiated immunity testing an overview of the reverberation chamber," *Proceedings of the 1998 South African Symposium on Communications and Signal Processing*, pp. 471-474, 1998.
- [3] IEC 61000-4-21, "Electromagnetic compatibility (EMC): testing and measurement techniques-reverberation chamber test methods," edition 2.0, Geneva, January 2011.
- [4] P. Corona, J. Ladbury, and G. Latmiral, "Reverberation-chamber research-then and now: a review of early work and comparison with current understanding," *IEEE Trans. on EMC*, vol. 44, no. 1, pp. 87-94, August 2002.
- [5] D. A. Hill, "Electromagnetic theory of reverberation chambers," *National Institute of Standards and Technology, US Department of Commerce, CO, NIST*, 1998.
- [6] P. Corona, J. Ladbury, and G. Latmiral, "Reverberation-chamber research-then and now: a review of early work and comparison with current understanding," *IEEE Trans. on EMC*, vol. 44, no. 1, pp. 87-94, August 2002.
- [7] T. A. Loughry, "Frequency stirring: an alternate approach to mechanical mode-stirring for the conduct of electromagnetic susceptibility testing," *Phillips Laboratory, Kirtland Air Force Base, NM*, November 1991.
- [8] Y. Huang and D. Edwards, "A novel reverberating chamber: the source-stirred chamber," *IEEE Eighth Int. Conf. on EMC*, Edinburgh, pp. 120-124, September 1992.
- [9] Y. Shen, D. Shi, Y. Gao, H. Y. Liu, and S. L. Liu, "Improvement in field uniformity introduced by multiple-antenna in source-stirred reverberation chamber," *Chinese Jour. of Radio Science*, vol. 24 no. 1, pp. 682-686, September 2009.
- [10] G. Cerri, C. Sanctis, V. Primiani, C. Monteverde, and P. Russo, "Array of antennas design for the source stirring technique," *IEEE 20<sup>th</sup> Int. Symp. On EMC*, Zurich, pp. 105-108, January 2009.
- [11] C. Bruns, "Three-dimensional simulation and experimental verification of a reverberation chamber," *Universitat Fridericiana Karlsruhe (TH)*, Germany, 2005.
- [12] W. Li, C. Yue, W. Yu, and Y. Mao, "Design and investigation of source-stirred reverberation chamber based on array antennas," *The 30th Int. Review of Progress in Applied Computational Electromagnetics*, CA, March 2013.
- [13] D. Hill, "Spatial correlation function for fields in a reverberation chamber," *IEEE Trans. on EMC*, vol. 37, no. 1, pp. 138, February 1995.

- [14] C. Bruns and R. Vahldieck, "A closer look at reverberation chambers-3D simulation and experimental verification," *IEEE Transactions on Electromagnetic Compatibility*, vol. 47, issue 3, 2005.
- [15] S. Liang, J. Xun, and J. Ding, "Investigation of antennas layout in the source stirred reverberation chamber," *Measurement & Control Technology*, vol. 30, issue 1, 2011.
- [16] V. M. Primiani, P. Russo, and G. Cerri, "Experimental characterization of a reverberation chamber excited by the source stirring technique," *2012 International Symposium on Electromagnetic Compatibility (EMC EUROPE)*, pp. 1-6, 2012.



**Wenxing Li** received his B.S. and M.S. degrees from Harbin Engineering University (HEU), Harbin, China, in 1982 and 1985, respectively. He is currently a Full Professor of the College of Information and Communication Engineering at HEU, China. He is

also the Head of Research Centre of EM Engineering & RF Technology. He visited the Department of Electrical Engineering, Pennsylvania State University, USA, from June to August 2010. And he visited Oriental Institute of Technology, Taiwan, from August to October 2010. He is also the organizer of the 30th Progress in Electromagnetics Research Symposium (PIERS), IEEE International Workshop on Electromagnetics (iWEM), TPC of 2012 Asia-Pacific Symposium on Electromagnetic Compatibility (APEMC 2012) and 2012 Global Symposium on Millimeter Waves (GSMM 2012). His recent research interests are mainly in computational electromagnetic, microwave engineering, modern antenna design and microwave and millimeter wave circuits.



**Chongyi Yue** received his B.S. and M.S. degrees from Harbin Engineering University, Harbin, Heilongjiang, China, in 2010 and 2012, respectively. He is currently working towards the doctor's degree in Information and Communication Engineering at Harbin Engineering

University in China. His research interests include source stirring reverberation chamber, computational electromagnetics and design of antenna array.



**Wenhua Yu** joined the Department of Electrical Engineering of the Pennsylvania State University, and has been a group leader of electromagnetic communication lab since 1996. He received his Ph.D. in Electrical Engineering from the Southwest

Jiaotong University in 1994. He worked at Beijing Institute of Technology as a Postdoctoral Research Associate from February 1995 to August 1996. He has published one book on CFDTD software and two FDTD books: *Conformal Finite-Difference Time-Domain Maxwell's Equations Solver: Software and User's Guide* (Artech House, 2003), *Parallel Finite-Difference Time-Domain* (CUC Press of China, 2005, in Chinese), and *Parallel Finite-Difference Time-Domain Method* (Artech House, 2006). He has published over 100 technical papers and four book chapters. He created the Computer and Communication Unlimited Company (<http://www.2comu.com>), and serves as its President. He is a Senior Member of the IEEE. He was included in Who's Who in America, Who's Who in Science and Engineering, and Who's Who in Education. He is also a Visiting Professor and Ph.D. Advisor of the Communication University of China. Yu's research interests include computational electromagnetic, numerical techniques, parallel computational techniques, and the theory and design of parallel computing systems.